REPORT DOCUMENTATION PAGE

Form Approved
OMB No. 0704-0188

1. REPORT DATE *(DD-MM-YYYY)*
22-04-2005

2. REPORT TYPE
Journal Article

3. DATES COVERED *(From - To)*

4. TITLE AND SUBTITLE

Performance testing of a microfabricated propulsion system for nanosatellite applications (POSTPRINT)

5a. CONTRACT NUMBER

5b. GRANT NUMBER

5c. PROGRAM ELEMENT NUMBER

6. AUTHOR(S)
Andrew D. Ketsdever (AFRL/PRSA); Riki H. Lee and Taylor C. Lilly (USC)

5d. PROJECT NUMBER
50260568

5e. TASK NUMBER

5f. WORK UNIT NUMBER

7. PERFORMING ORGANIZATION NAME(S) AND ADDRESS(ES)

Air Force Research Laboratory (AFMC)
AFRL/PRSA
10 E. Saturn Blvd.
Edwards AFB CA 93524-7680

8. PERFORMING ORGANIZATION REPORT NUMBER

AFRL-PR-ED-JA-2005-132

9. SPONSORING / MONITORING AGENCY NAME(S) AND ADDRESS(ES)

Air Force Research Laboratory (AFMC)
AFRL/PRS
5 Pollux Drive
Edwards AFB CA 93524-7048

10. SPONSOR/MONITOR'S ACRONYM(S)

11. SPONSOR/MONITOR'S NUMBER(S)
AFRL-PR-ED-JA-2005-132

12. DISTRIBUTION / AVAILABILITY STATEMENT

Approved for public release; distribution unlimited

13. SUPPLEMENTARY NOTES
As published in Journal of Micromechanics and Microengineering, 15 (2005) 2254-2263.

14. ABSTRACT
There is a growing interest in the use of micro and nanosatellites within the aerospace community. Constellations of small satellites may eventually replace much larger, single function spacecraft as a cheaper, more flexible alternative. Micro-technologies will be required to enable small satellite missions including efficient, low-cost propulsion systems for maneuvering. A MEMS fabricated propulsion system has been developed for maneuvers on an upcoming University nanosatellite mission. The Free Molecule Micro-Resistojet (FMMR) is an electrothermal propulsion system designed for on-orbit maneuvers of nanosatellites, which are defined as spacecraft with an initial mass less than 10 kg. The FMMR has been tested using a torsion force balance to assess its performance using a variety of propellants including helium, argon, nitrogen and carbon dioxide. The experimental performance results compare favorably with results obtained from gas kinetic theory, which were used in the design phase to estimate the thruster's performance. The measured performance of the FMMR in this study has proven to be adequate to perform attitude control maneuvers for the University nanosatellite mission.

15. SUBJECT TERMS

16. SECURITY CLASSIFICATION OF: a. REPORT	b. ABSTRACT	c. THIS PAGE	17. LIMITATION OF ABSTRACT	18. NUMBER OF PAGES	19a. NAME OF RESPONSIBLE PERSON
Unclassified	**Unclassified**	**Unclassified**	A	11	Dr. Ingrid J. Wysong
					19b. TELEPHONE NUMBER *(include area code)* (661) 275-5206

Standard Form 298 (Rev. 8-98)
Prescribed by ANSI Std. 239.18

INSTITUTE OF PHYSICS PUBLISHING JOURNAL OF MICROMECHANICS AND MICROENGINEERING

J. Micromech. Microeng. **15** (2005) 2254–2263 doi:10.1088/0960-1317/15/12/007

Performance testing of a microfabricated propulsion system for nanosatellite applications

Andrew D Ketsdever[1], Riki H Lee[2] and Taylor C Lilly[2]

[1] Propulsion Directorate, US Air Force Research Laboratory, 10 E Saturn Blvd, Edwards Air Force Base, CA 93524, USA

[2] Department of Aerospace and Mechanical Engineering, University of Southern California, 854 W 36th Place, RRB 101, Los Angeles, CA 90089-1191, USA

E-mail: ketsdeve@usc.edu

Received 23 May 2005, in final form 10 October 2005
Published 28 October 2005
Online at stacks.iop.org/JMM/15/2254

Abstract

There is a growing interest in the use of micro and nanosatellites within the aerospace community. Constellations of small satellites may eventually replace much larger, single function spacecraft as a cheaper, more flexible alternative. Micro-technologies will be required to enable small satellite missions including efficient, low-cost propulsion systems for maneuvering. A MEMS fabricated propulsion system has been developed for maneuvers on an upcoming University nanosatellite mission. The Free Molecule Micro-Resistojet (FMMR) is an electrothermal propulsion system designed for on-orbit maneuvers of nanosatellites, which are defined as spacecraft with an initial mass less than 10 kg. The FMMR has been tested using a torsion force balance to assess its performance using a variety of propellants including helium, argon, nitrogen and carbon dioxide. The experimental performance results compare favorably with results obtained from gas kinetic theory, which were used in the design phase to estimate the thruster's performance. The measured performance of the FMMR in this study has proven to be adequate to perform attitude control maneuvers for the University nanosatellite mission.

(Some figures in this article are in colour only in the electronic version)

1. Introduction

Recent trends in the space community for smaller, cheaper and more frequent space missions have driven the development of micro and nanosatellites. The use of small spacecraft constellations is an attempt to enhance the overall performance of communication and remote sensing tasks currently done by a relatively small number of large platforms [1, 2]. Because micro-technologies have the advantage of reducing the total resources required on a spacecraft, the continued development of micro-technologies for space applications will further enable small satellite missions [3, 4]. Nanosatellites (mass between 1 and 10 kg) impose significant limitations on mass, power and volume available for all subsystems including propulsion [5]. In general, micropropulsion devices will need to be more efficient, in an overall systems architecture sense, than their large spacecraft counterparts in order to maximize the limited resources available. For micropropulsion systems, MEMS fabrication processes can be used to integrate thrusters, valves and control electronics into a single device in an attempt to provide a high degree of system efficiency. To this end, the Free Molecule Micro-Resistojet (FMMR) has been developed by the Air Force Research Laboratory.

The FMMR is an electrothermal propulsion system [6] designed for on-orbit maneuvers of nanosatellites. As with any resistojet, the propellant flow through the FMMR is heated by passing it over an electrically heated surface. The FMMR consists of three main parts: the heater chip, the plenum and the propellant feed system as shown in figure 1. The thrust generating principle of the FMMR is shown in figure 2.

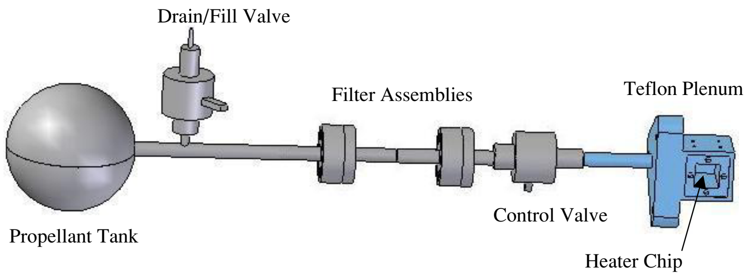

Figure 1. FMMR flight assembly schematic.

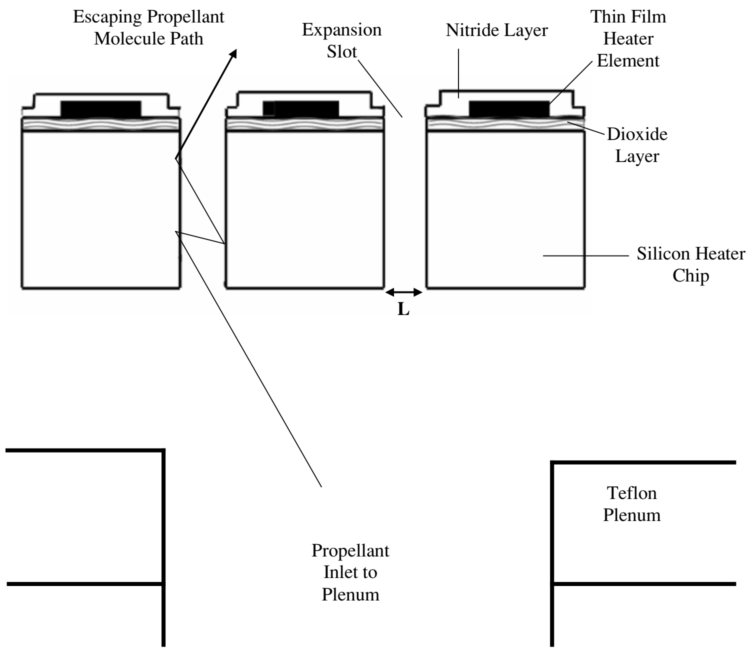

Figure 2. Basic thrust generation principle of the FMMR.

The propellant gas arrives in the plenum after passing from the propellant storage tank through the propellant feed system. The propellant gas escapes the plenum through a series of expansion slots in the MEMS fabricated heater chip, thus generating thrust. The heater chip is designed to operate at temperatures up to 600 K. The propellant molecules gain kinetic energy as they collide with the heated walls of the expansion slots in the heater chip. The transfer of energy from the high temperature expansion slot wall to the propellant molecules is critical to the performance and operation of the FMMR, since the thrust and efficiency, as measured by the specific impulse, of a propulsion system vary linearly with the propellant molecule's velocity at the exit of the thruster.

The FMMR exhibits many system features that are beneficial to nanosatellite operations, such as low-pressure operation, low power consumption, low mass and low propellant storage volume. Low-pressure operation is beneficial for micropropulsion systems for two main reasons. First, valve leak rates are dependent on the operating pressure. Valve leak rate concerns can be reduced for the FMMR over systems that operate at high pressures. This is particularly important when considering MEMS fabricated valves since many state-of-the-art valve designs will not meet nanosatellite mission requirements [7]. Second, the FMMR can be operated on the vapor pressure of a propellant stored as either a liquid or solid at nominal storage temperatures. The storage density of the propellant is important to minimize the volume required for propellant tanks.

Another distinct benefit of the FMMR propulsion system is expansion of propellant gases through many long slots. The expansion slot design leads to a reduction in possible single point failures over the expansion of propellant through a single nozzle configuration, which is a more traditional thruster design. To produce a similar amount of thrust as the FMMR using a high-pressure nozzle expansion, the throat diameter of the nozzle would be relatively small. Plugging of the throat by a contaminant would lead to a failure; however, the plugging of a section of slot in the FMMR device would still leave the remaining slot area available for thrust generation. A potential drawback of the expansion slot design is the loss of propulsive efficiency. However, a previous study has shown that for low-pressure operation, a nozzle does not offer a distinct enhancement in performance over a simple orifice or slot [8].

The aim of this research was to assess the thermal and propulsive performance characteristics of the FMMR

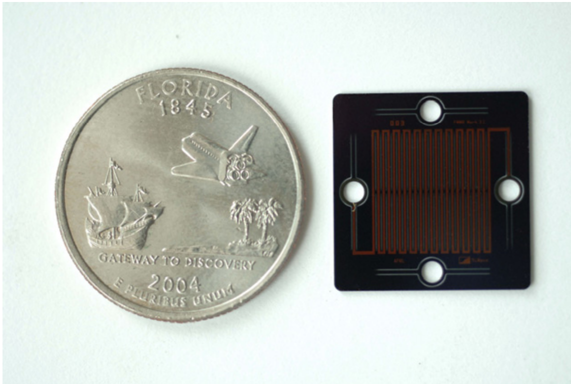

Figure 3. MEMS fabricated heater chip.

Table 1. Nanosatellite propulsion system requirements.

Parameter	Budget/requirement
Power	
Steady state	5 W
Transient	9 W
Propellant mass	90 g
Propellant volume	100 cm^3
Thrust	8×10^{-4} N

Mark 3.1 operating on several different propellants. This version of the FMMR was specifically developed to provide attitude control for an upcoming University nanosatellite mission. The FMMR will provide a de-spin capability for the nanosatellite to allow proper positioning of the satellite. The propulsive requirements for the nanosatellite mission are given in table 1. A slightly different version of the FMMR heater chip was integrated to an Arizona State University nanosatellite that was launched on the inaugural Delta-IV heavy launch vehicle in December 2004. Unfortunately, the 3-Corner Sat nanosatellite did not reach orbit due to a launch vehicle anomaly. In addition to the flight on an upcoming nanosatellite, the current version of the FMMR will be launched on a suborbital flight onboard a newly developed launch vehicle [9].

2. Microfabrication

The FMMR Mark 3.1 heater chip is shown in figure 3. The current iteration of the FMMR heater chip is a 19.2 mm × 19.2 mm square. The heater chip is fabricated using standard MEMS processing techniques. Individual heater chips are fabricated from a 500 μm thick double-sided polished silicon wafer which has been oxidized with a 0.4 μm layer of thermal oxide. The oxide acts as an electrical insulator between the silicon substrate and the subsequently deposited thin-film heater. The fabrication can be divided into the thin-film heater metallization and the deep reactive ion etching (DRIE) steps. Metallization of the heaters begins with a 0.03 μm layer of titanium which acts as an adhesion layer between the oxide layer and the subsequent metal layers. A 0.06 μm layer of platinum is then deposited to act as a diffusion barrier to mobile ions. A final layer of gold is deposited and provides the main current carrying layer of the heating element. The resistance of the gold layer, which is dictated by the layer thickness of 0.075 μm, was selected to allow the heater chip to reach the desired operating temperature while being supplied by the fixed satellite bus voltage for the nanosatellite mission. The heater is patterned to run between each expansion slot in an attempt to keep the heater chip temperature uniform. Once the metallization of the heater is completed, the wafer and patterned metallization is nitride coated in order to encapsulate the heating element, providing an isolation and scratch resistant layer.

The DRIE step was used to fabricate the expansion slots, thermal compensating flexures, attachment holes and was used to pattern the individual heater chips on the wafer. The expansion slots are anisotropically etched using the DRIE technique, which was selected to achieve the desired high aspect ratio. There are 44 expansion slots formed in two rows on each heater chip separated by a small rib to insure structural stability. The FMMR heater chip was specifically designed to survive the expected vibrational and g-force loading expected during the launch of the nanosatellite. The slots are 100 μm wide and 5.375 mm long and etched completely through the 500 μm thick wafer as shown in figure 4. The thrust generated by the FMMR is directly proportional to the collective expansion slot area for a given operating pressure. Therefore, the FMMR can be tailored to meet several different mission requirements by adjusting the expansion slot area.

The DRIE process is also used to fabricate thermal compensator flexures around the attachment holes that are used to attach the heater chip to the plenum. Since the heater chip operates nominally at temperatures of 600 K, the flexures are necessary to account for differential thermal expansion between the heater chip and the cooler plenum. The FMMR is currently packaged by attaching the MEMS fabricated heater chip to a conventionally machined plenum and propellant feed system. Figure 5 shows the heater chip attached to a Teflon plenum assembly that was tested in this study. The Teflon plenum is used to minimize heat transfer and keep the power required for the heater chip as low as possible. In future iterations, integration of the heater chip with other MEMS components and full MEMS packaging techniques must be investigated to improve system efficiency and integration.

3. Theory

The performance of the FMMR is analyzed theoretically as the free molecule flux of mass and momentum through the expansion slots. The amount of rarefaction in a flow is measured by the Knudsen number:

$$Kn = \frac{\lambda}{L} = \frac{1}{\sqrt{2}n\sigma L}, \tag{1}$$

where λ is the molecular mean free path (the average distance that a molecule travels before colliding with another molecule), L is a characteristic flow dimension (the expansion slot width in this case), n is the number density of the propellant in the plenum and σ is the collision cross-section for the propellant molecules. Free molecule conditions are defined by $Kn \gg 1$ where either the mean free path is very large or the characteristic dimension is very small. Since the FMMR is designed to operate in the transitional flow regime with a

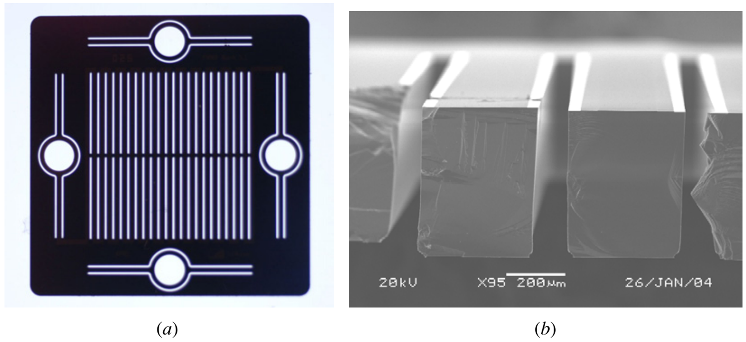

Figure 4. (*a*) Expansion slot configuration on the heater chip. (*b*) Scanning electron microscope side image of cleaved expansion slots.

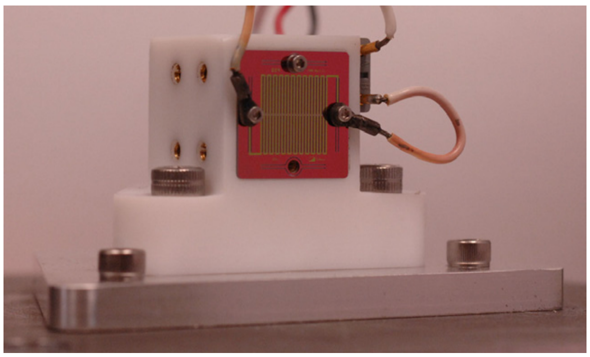

Figure 5. MEMS fabricated heater chip and Teflon flight plenum.

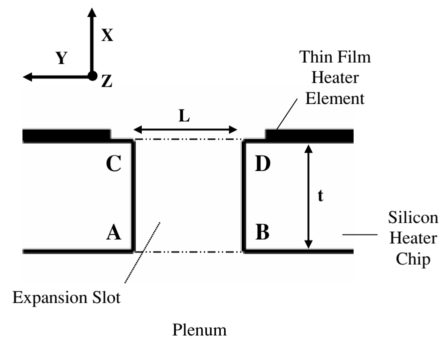

Figure 6. Expansion slot nomenclature and coordinate system.

Knudsen number range between 0.1 and 1, the free molecule analysis that follows is expected to only be approximate. However, the analysis has proven useful in the initial design phase of the FMMR.

The flux per unit area of a molecular parameter Q (either mass, momentum or energy) through a surface is given by

$$\dot{Q} = \int_{-\infty}^{\infty}\int_{-\infty}^{\infty}\int_{0}^{\infty} Q v'_x f(v'_x)\,\mathrm{d}v'_x\,\mathrm{d}v'_y\,\mathrm{d}v'_z, \tag{2}$$

where v'_x is the average thermal speed of the molecule in the x-direction and $f(v'_x)$ is the Maxwellian velocity distribution function for a gas in thermodynamic equilibrium [10]. Equation (2) assumes an orthogonal coordinate system with x in the direction of flow parallel with the expansion slot thickness and the expansion slot entrance and exit in the y–z plane as shown in figure 6.

The mass flux can be derived using equation (2) by setting $Q = \alpha m n$ where m is the mass of the propellant molecules and α is a transmission probability. The transition probability is defined as the probability that a propellant molecule which enters an expansion slot (i.e., crosses line AB in figure 6) will leave the thruster exit plane (i.e., cross line CD in figure 6) and produce thrust. For an infinitely thin expansion slot or for specular wall collisions, the value of the transmission probability would be unity. For the slot thickness to width ratio used in the present FMMR geometry ($t/L = 5$), the transmission probability assuming diffuse wall collisions is approximately 0.38 [11]. This value agrees well with published results for conductance through rectangular slots with similar t/L [12]. The mass flux of propellant molecules through an expansion slot is

$$\dot{m} = \alpha m n \frac{\bar{v}'}{4} A_s, \tag{3}$$

where $\bar{v}'$ is the average thermal speed of the propellant molecules in the plenum and A_s is the expansion slot area. The average thermal speed of the propellant molecules is given by the expression

$$\bar{v}' = \sqrt{\frac{8kT_o}{\pi m}}, \tag{4}$$

where k is Boltzmann's constant and T_o is the temperature of the propellant molecules in the plenum. Combining equations (3) and (4) with the ideal gas law results in

$$\dot{m} = \alpha P_o \sqrt{\frac{m}{2\pi k T_o}}\, A_s, \tag{5}$$

where P_o is the pressure of the propellant gas in the plenum.

The thrust generated by the propellant gas expanding through the slots can be defined in a high Mach number flow as

$$\Im = \dot{m} u_e, \tag{6}$$

where u_e is the propellant velocity at the exit plane of the expansion slot. The exit velocity can be derived from free molecule flow as

$$u_e = \sqrt{\frac{\pi k T_w}{2m}}, \tag{7}$$

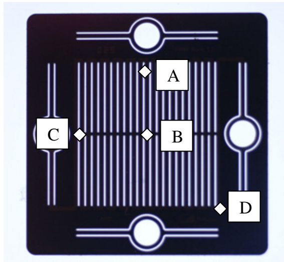

Figure 7. Thermocouple positions on the FMMR heater chip. Unless otherwise noted, the heater chip temperature was measured at position A.

where T_w is the heated wall temperature of the expansion slot. Therefore, the theoretical thrust produced by the FMMR can be written as

$$\Im = \frac{\alpha P_o A_s}{2}\sqrt{\frac{T_w}{T_o}}. \quad (8)$$

The specific impulse or Isp is used as a measure of the propellant utilization efficiency and is defined as

$$\mathrm{Isp} = \frac{\Im}{\dot{m} g_o} = \frac{u_e}{g_o} = \sqrt{\frac{\pi k T_w}{2 m g_o^2}}, \quad (9)$$

where g_o is the Earth's gravitational acceleration. As can be seen in equation (9), the Isp is inversely proportional to the square root of the propellant molecular mass; therefore, lighter propellant molecules will result in increased propellant efficiency. The FMMR has been designed to operate using water propellant with a relatively low molecular weight that can be stored as a liquid or solid. The Isp is also proportional to the square root of the wall temperature; therefore, higher wall temperatures will result in better propellant efficiency. However, the operating heater chip temperature must be weighed against the required power.

The overall efficiency of an electric propulsion system is measured by the product of the thrust and specific impulse per unit input power as given by

$$\eta = \frac{\Im \,\mathrm{Isp}\, g_o}{2\wp} = \frac{\Im^2}{2\dot{m}\wp}, \quad (10)$$

where $\wp$ is the input power to the heater chip. Based on this formulation, large-scale resistojets generally have efficiencies on the order of 25–35% [13].

4. Experimental set-up

After the fabrication of the heater chip and plenum, the FMMR was tested to assess its thermal properties. For nanosatellite operations, the input power to the heater chip will be extremely limited. For efficient operation of the FMMR, the input power must couple efficiently to the propellant gas through collisions with the expansion slot walls. The heat transfer characteristics of the FMMR design were measured using a series of thermocouples attached to various parts of the heater chip and plenum. The locations of the thermocouples on the heater chip are shown in figure 7. The FMMR was placed in a vacuum chamber with an ultimate background pressure capability of 10^{-6} Torr. Transient and steady-state temperature measurements were recorded as a function of input power and propellant mass flow. The final step of this process involved placing the FMMR under a liquid nitrogen shield to simulate temperatures that a nanosatellite might encounter on-orbit. Similar data sets were recorded for background temperatures of 120 K and 300 K.

Table 2. Nominal FMMR operating parameters.

Parameter	Value
Heater chip temperature, T_w	600 K
Mass flow, $\dot{m}$	50 sccm
Plenum pressure, P_o	
Helium	35 Pa
Nitrogen	95 Pa
Argon	112 Pa
Carbon dioxide	120 Pa

The propulsive characteristics of the FMMR were measured using the nano-Newton thrust stand (nNTS) and an electrostatic comb calibration system described in detail elsewhere [14, 15]. The nNTS was placed in a large vacuum chamber, Chamber IV of the Collaborative High Altitude Flow Facility at the University of Southern California, which was capable of maintaining background pressures below 10^{-5} Torr throughout the range of experiments performed in this study. Maintaining low background pressure was critical in obtaining accurate thrust measurements [16]. The mass flow of propellants was measured along with the thrust in order to determine the thruster's specific impulse. Tests were conducted using helium, nitrogen, carbon dioxide and argon propellants. Mass flow rates of the propellants ranged from 1 to 100 sccm, and heater chip temperatures ranged from 300 to 600 K. Unless otherwise noted, the heater chip temperature is measured from the thermocouple at position A (figure 7). For the upcoming nanosatellite mission, the nominal operating characteristics of the FMMR are given in table 2.

5. Results and discussion

The requirements for maximum allowable power draw and minimum allowable thrust generated from the onboard propulsion system make the efficiency of the FMMR a critical design component for this mission. The propulsive efficiency is given by equation (10) and is seen to be a trade-off between higher thrust (with a higher heater chip temperature) and the increased power required to generate that thrust. To establish that the current FMMR design meets both the transient and steady-state power requirements, experiments were performed to measure thermal characteristics of the heater chip and plenum assembly.

The heater chip temperature as a function of input power is shown in figure 8 for various propellants with a constant mass flow rate of 50 sccm. The nominal operating temperature of the FMMR heater chip of 600 K was obtained with an input power of 3.7 W at the nominal propellant mass flow of 50 sccm. The input power required to heat the heater chip to 600 K is shown in figure 8 to be relatively independent of the propellant gas used for a given propellant number flux (mass flow in sccm). An empirical formulation was derived to estimate the input power required to heat the heater chip to a given temperature

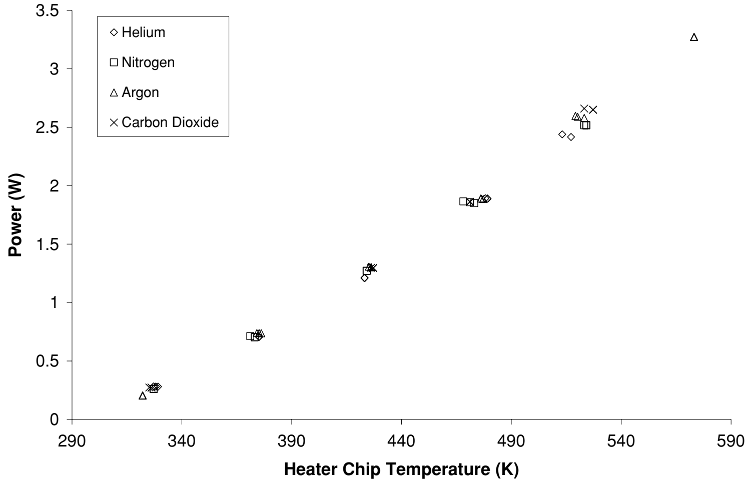

Figure 8. Heater chip temperature as a function of thin-film heater input power.

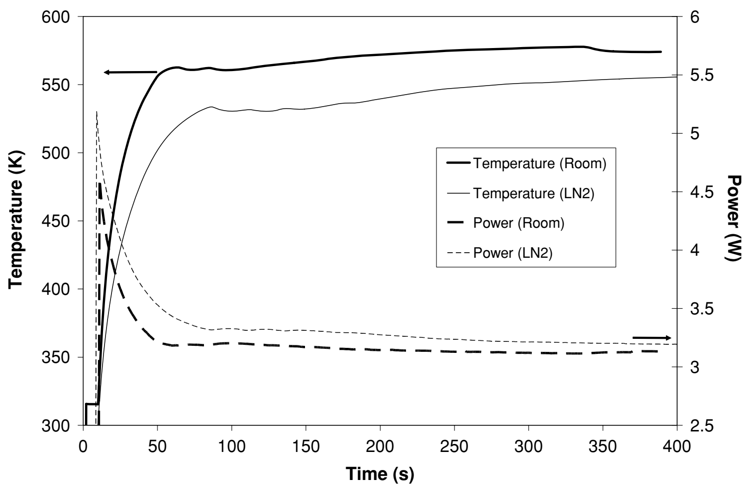

Figure 9. Transient heater chip temperature and input power for the heater chip radiating to the vacuum chamber walls (room temperature, 300 K) and to a liquid nitrogen shield (120 K).

Table 3. Empirical constants for equation (11).

Empirical constant	Value
a_1	1.279×10^{-5}
a_2	8.647×10^{-4}
a_3	-1.401
c_1	2.005×10^{-3}
c_2	0.9003

as a function of the propellant mass flow. The empirical result is given by

$$\wp = \left(a_1 T_w^2 + a_2 T_w + a_3\right)(c_1 \dot{m} + c_2), \tag{11}$$

where T_w is the heater chip temperature in Kelvin and $\dot{m}$ is the propellant mass flow in sccm. The empirical constants in equation (11) are given in table 3. Equation (11) is valid for all of the propellants used in this study. The transient heat transfer properties of the FMMR are shown in figure 9. The two cases investigated were for the heater chip radiating to a wall at 300 K (room) and a wall at 120 K (LN2). For a constant input voltage applied to the thin-film heater at time $t = 0$, the power draw and corresponding heater chip temperature are shown with no propellant mass flow. For efficient FMMR operation, the heater chip will be brought to steady-state operating temperature before the propellant mass flow is initiated. Based on figure 9, a time between 60 and 100 s is required to bring the FMMR to steady-state operating temperature depending on the initial temperature of the heater chip. Although the nominal steady-state input power is on the order of 3.25 W in figure 9, a transient input power as high as 5.25 W is present for a short time at start-up. This is due to the relatively low thin-film heater resistance at low temperature. The heater resistance increases with temperature, which acts to lower the input power at constant voltage. For a power limited nanosatellite system, the initial spike in the FMMR power draw could be an issue that must be addressed in the power budget. The transient and steady-state power requirements for the nanosatellite mission are given in table 1.

The uniformity of the temperature across the heater chip is important in establishing efficient operation. The nominal

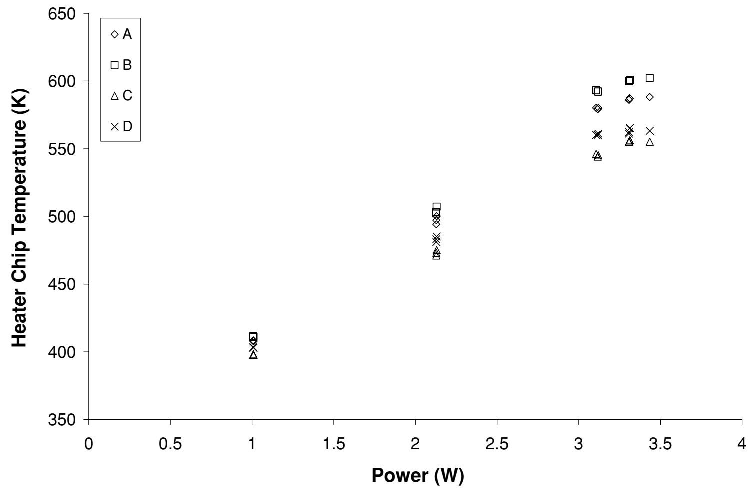

Figure 10. Heater chip temperature as a function of thin-film heater input power at various positions on the heater chip.

operating temperature of the FMMR heater chip is 600 K, which is the desired temperature at the center of the heater chip (position B in figure 7). The design criterion was for the heater chip temperature at any point to be within 10% of the temperature at the center. Figure 10 shows the heater chip temperature as a function of input power for various locations on the heater chip. As seen in figure 10 for an argon propellant with a mass flow of 50 sccm, the heater chip temperature remained within 3% of the center temperature at the lowest power setting and within 8% in the higher power range. Similar results were obtained for all of the propellants and corresponding mass flow rates investigated in this study. The subsequent values of the heater chip temperature, T_w, are given for position A where the temperature was monitored for the thrust testing.

Figure 11(a) shows the propellant mass flow as a function of the FMMR plenum pressure for various propellants at a constant $T_w = 575$ K. Figure 11(b) shows the data for helium compared to the theoretical line obtained from equation (5). There are several explanations for the differences between theory and experiments. One possibility is the uncertainty of the fabricated expansion slot area. A second possibility is the flow regime of the experiments. As figure 11(b) shows, the operating regime of the FMMR provides a higher mass flow rate than the free molecule theory predicts. Recall that the theory developed earlier assumed free molecule flow with $Kn \gg 1$. For the pressure range in figure 11(b), the helium Knudsen number ranged from 3 to 40. This is classified as the transitional flow regime [10] for which there are no analytical solutions of the Boltzmann equation. The low Knudsen numbers imply that the FMMR flows for these conditions are not free molecular, and there are a significant number of collisions between propellant molecules. As the FMMR plenum pressure increases even more, a continuum flow regime is approached ($Kn \ll 1$), and the transport of mass through the expansion slots is expected to become more efficient [8]. However for the FMMR, there is expected to be a trade-off between increased mass flow and the overall propulsive efficiency. As the mass flow increases (increased plenum pressure leading to a decrease in flow Knudsen number), intermolecular collisions will increase and a boundary layer will form near the expansion slot wall. The boundary layer will act to decrease the ability of the expansion slot wall to heat the gas outside of the boundary layer. Much of the propellant gas will exit the expansion slot without having increased its kinetic energy through collisions with the heated walls.

Table 4. Curve fit equations for figures 13 and 14(a).

Figure	Propellant gas	Curve fit equation	R^2
13	He	$Y = 1.505 \times 10^{-5}\, x^{0.4143}$	0.9992
13	N_2	$y = 2.506 \times 10^{-5}\, x^{0.5046}$	0.9995
13	Ar	$y = 3.185 \times 10^{-5}\, x^{0.4877}$	0.9998
13	CO_2	$y = 4.862 \times 10^{-5}\, x^{0.4335}$	0.9979
14(a)	He	$y = 9.395\, x^{0.4431}$	0.9993
14(a)	N_2	$y = 3.054\, x^{0.4788}$	0.9990
14(a)	Ar	$y = 2.424\, x^{0.4836}$	0.9997
14(a)	CO_2	$y = 2.615\, x^{0.4737}$	0.9994

Figure 12 shows the thrust obtained by the nano-Newton thrust stand as a function of the propellant mass flow rate. The results in figure 12 are for various propellants at $T_w = 575$ K. This is expected to be a linear relationship based on equation (6) since the exit velocity should be constant for a constant heater chip temperature. Figure 13 shows the thrust as a function of T_w for a constant $\dot{m} = 50$ sccm. From equation (8), the relationship between thrust and heater chip temperature is expected to vary as $\sqrt{T_w}$. The curve fit (best fit) equations for the data in figure 13 is given in table 4. Figure 14(a) shows the specific impulse as a function of T_w for a constant $\dot{m} = 50$ sccm for a variety of propellants. Figure 14(b) shows the specific impulse data for helium compared to the free molecule theory result from equation (9). Differences between theory and experiment in figure 14 may stem from a variety of uncertainties and approximations including the assumption of high Mach number flow that stems from the use of equation (6). As with the thrust data, the specific impulse is expected to vary as $\sqrt{T_w}$. The curve fit (best fit) equations for the data in figure 14 are also given in table 4. As expected, the measured specific impulse is greater than that

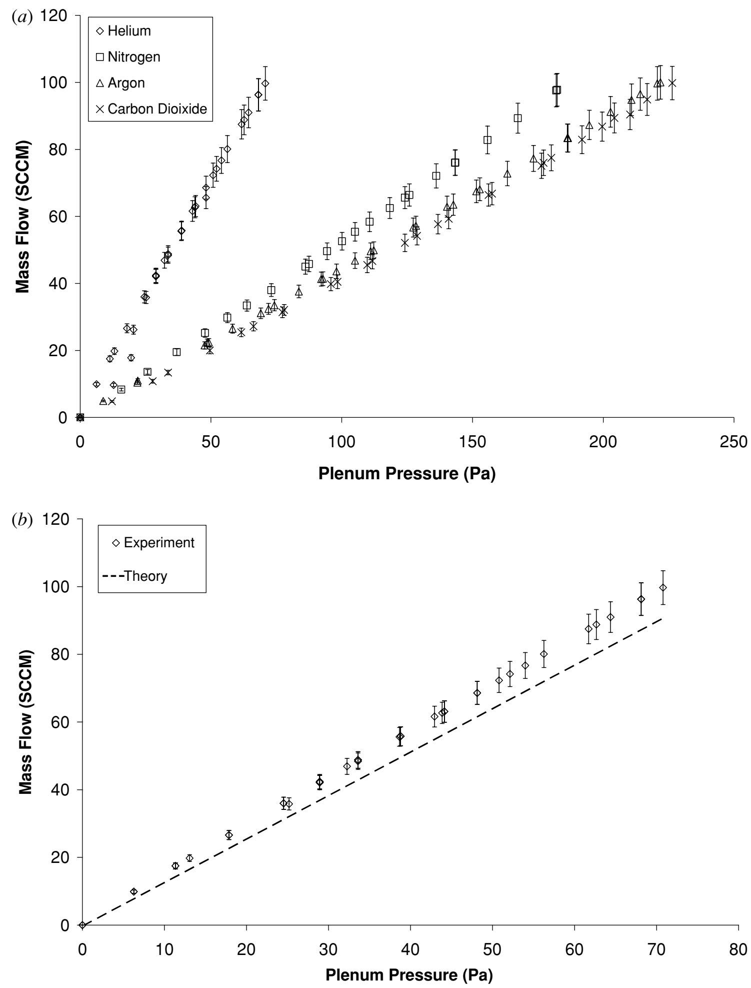

Figure 11. Mass flow versus plenum pressure for (*a*) various propellants. (*b*) Helium compared with free molecule theory.

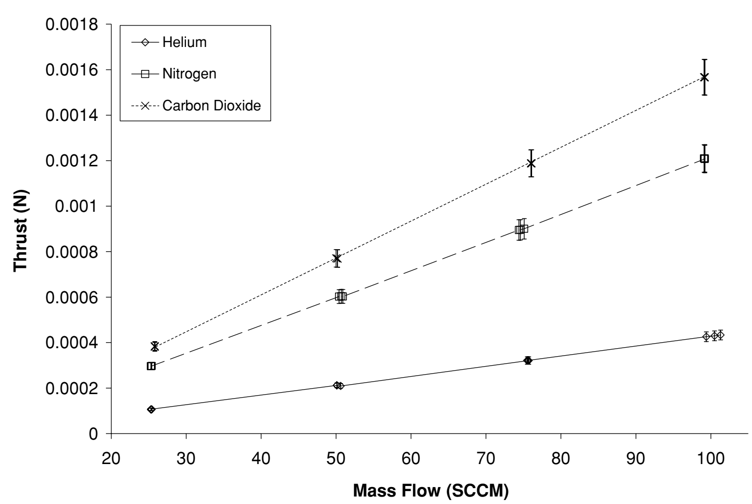

Figure 12. Thrust versus mass flow for various propellants.

predicted by the free molecule theory due to the transitional flow regime selected for FMMR operations. Table 5 gives the current FMMR parameters with the associated requirements for the nanosatellite mission. In its current configuration, the FMMR system will meet all of the mission requirements for the nanosatellite mission.

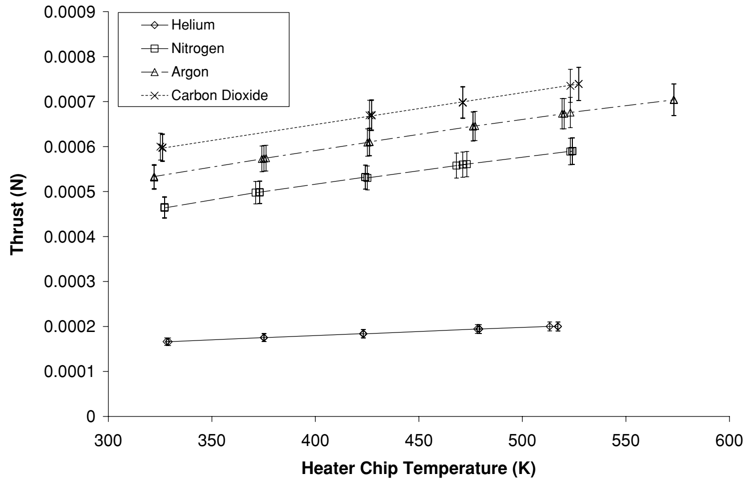

Figure 13. Thrust as a function of heater chip temperature for various propellants.

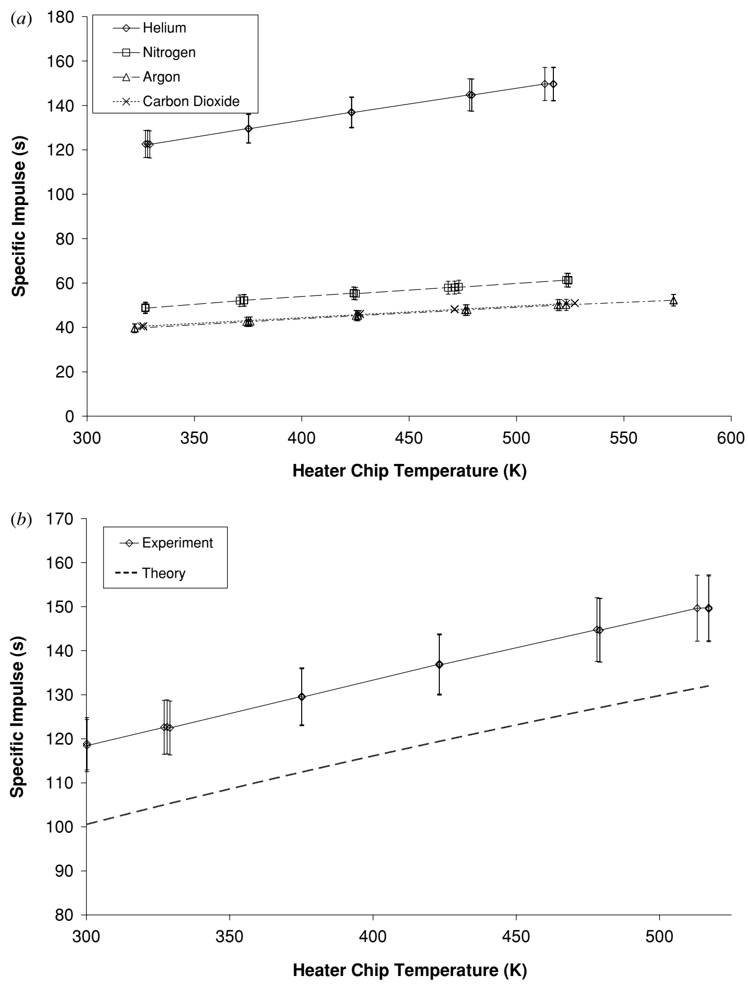

Figure 14. Specific impulse versus heater chip temperature for (*a*) various propellants. (*b*) Helium compared with free molecule theory.

The propulsive efficiency of the FMMR at nominal operating conditions (table 2) is approximately 15%. The efficiency is shown to improve up to 25% for higher mass flow rates at a given input power level. Increased efficiency can come from several different parameters. Minimizing the heat losses from the heater chip to the plenum would lead

Table 5. Comparison of nanosatellite mission requirements with the propulsive characteristics of the FMMR. The margin is the difference between the measured value and the requirement. Positive margin is required to meet (exceed) the requirements.

Parameter	Budget/ requirement	Measured values	Margin
Power			
Steady state (W)	5	3.2	+1.8
Transient (W)	9	5	+4
Propellant mass (g)	90	87	+3
Propellant volume (cm^3)	100	96	+4
Thrust (N)	8×10^{-4}	1.7×10^{-3}	$+9 \times 10^{-4}$

to an overall reduction in the total input power. This can be accomplished by minimizing the contact surface area of the heater chip with the surrounding plenum. The thrust produced by the FMMR can also be improved with the fabrication of more expansion slots per unit area. Efficiencies on the order of 30% could be possible with these relatively minor improvements to the current design.

From equation (9), it is evident that the specific impulse of the FMMR can be improved by using propellants with low molecular mass. Storing high-density propellants (either solid or liquid) also has distinct advantages in reducing the storage volume required over gaseous propellants stored at high pressure. To improve the overall system efficiency of the FMMR, a water vapor propellant is being investigated [17]. Water has many attractive benefits as a propellant such as liquid (or solid) storage on orbit and a relatively low molecular mass. Preliminary measurements and numerical simulation suggest that a specific impulse of approximately 68 s can be attained using water vapor at the FMMR nominal operating conditions. In this configuration, the FMMR would operate on the vapor pressure of the liquid water.

6. Conclusions

A simple method of fabricating a novel MEMS propulsion system has been demonstrated. The effects of propellant species, propellant mass flow and heater chip input power on the thermal and propulsive properties of the FMMR have been investigated. The propulsive properties of the FMMR were tested using a nano-Newton thrust stand. Data for propellant mass flow, thrust and specific impulse follow the trends predicted from free molecule theory. Although the absolute values differ, this was expected since the flows investigated in this study were in the transitional regime and not strictly free molecular. Thrust varied linearly with plenum pressure and mass flow at a constant T_w as expected. For a constant P_o, the thrust was relatively independent of the propellant gas used. For a constant propellant mass flow, the thrust varied approximately as $\sqrt{T_w}$. The specific impulse varied approximately as $\sqrt{T_w/m}$. Higher specific impulse was measured for larger T_w and propellants with a smaller molecular mass. At nominal operating conditions, the overall efficiency of the FMMR was approximately 15%. Optimizing the number of expansion slots per unit heater chip area and optimizing the heat transfer between the heater chip and the plenum can improve the overall efficiency of the FMMR for future nanosatellite missions. However, as shown in table 5, the FMMR system has positive margins for all of the mission requirements for the upcoming nanosatellite flight.

Acknowledgments

This work was supported by the Propulsion Directorate of the Air Force Research Laboratory at Edwards AFB, California. The authors wish to thank Mr Mike Huggins, Mr Jay Levine and Dr Ingrid Wysong for their continued support. The authors are also indebted to Dr Stephen Vargo of SiWave, Inc. for his efforts in assisting with the design and fabrication of the FMMR heater chip.

References

[1] Janson S, Helvajian H and Robinson E 1993 The concept of nanosatellite for revolutionary, low-cost space systems *44th International Astronautics Congress (Graz, Oct. 1993)* IAF Paper 93-U.5.573

[2] Bille M, Kane R and Nowlin M 2002 Military microsatellites: matching requirements and technology *Space 2000 Conference (Long Beach, CA, Sept. 2000)* AIAA Paper 2000-5186

[3] Martinez de Aragon A 1998 Space applications of micro/nano-technologies *J. Micromech. Microeng.* **8** 54–6

[4] Helvajian H 1997 *Microengineering Technology for Space Systems* (Reston, VA: AIAA)

[5] Ketsdever A D 2000 System considerations and design options for microspacecraft propulsion systems *Micropropulsion for Small Spacecraft* (Reston, VA: AIAA)

[6] Jahn R G 1968 *Physics of Electric Propulsion* (New York: McGraw-Hill)

[7] Mueller J 2000 Thruster options for microspacecraft: a review and evaluation of state-of-the-art and emerging technologies *Micropropulsion for Small Spacecraft* (Reston, VA: AIAA)

[8] Ketsdever A D, Clabough M T, Gimelshein S F and Alexeenko A A 2005 Experimental and numerical determination of micropropulsion device efficiencies at low Reynolds number *AIAA J.* **43** 633–41

[9] Ketsdever A D, D'Souza B, Jamison A J, Young M and Chinnery A 2002 Sub-orbital flight demonstration of MEMS technologies for space applications *NanoTech 2002 (Houston, TX, Sept. 2002)* AIAA Paper 2002-5704

[10] Bird G A 1994 *Molecular Gas Dynamics and the Direct Simulation of Gas Flows* (New York: Oxford University Press)

[11] Ketsdever A D, Green A A, Muntz E P and Vargo S E 2000 Fabrication and testing of the Free Molecule Micro-Resistojet: initial results *36th Joint Propulsion Conference (Huntsville, AL, July 2000)* AIAA Paper 2000-3672

[12] Lafferty J 1992 *Foundation of Vacuum Science and Technology* (New York: Wiley)

[13] Filliben J D 1997 *Electric Thruster Systems* CPTR 97-65 (Columbia, MD: Chemical Propulsion Information Agency)

[14] Jamison A J, Ketsdever A D and Muntz E P 2002 Gas dynamic calibration of a nano-Newton thrust stand *Rev. Sci. Instrum.* **73** 3629–37

[15] Selden N P and Ketsdever A D 2003 Comparison of force balance calibration techniques for the nano-Newton range *Rev. Sci. Instrum.* **74** 5249–54

[16] Ketsdever A D 2002 Facility effects on performance measurements of micropropulsion systems that utilize gas expansion *J. Prop. Power* **18** 797–804

[17] Ketsdever A D 2000 Predicted performance and systems analysis of the Free Molecule Micro-Resistojet *Micropropulsion for Small Spacecraft* (Reston, VA: AIAA)